



Revealing the Wonder of Natural Photonics by Nonlinear Optics

Dimitrije Mara ¹, Bojana Bokic ², Thierry Verbiest ³, Sébastien R. Mouchet ^{4,5,*} and Branko Kolaric ^{2,6,*}

- ¹ Institute of General and Physical Chemistry, Studentski trg 12/V, 11158 Belgrade, Serbia
² Center for Photonics, Institute of Physics, University of Belgrade, Pregrevica 118, 11080 Belgrade, Serbia
³ Molecular Imaging and Photonics, Department of Chemistry, KU Leuven, Celestijnenlaan 200D, 3001 Heverlee, Belgium
⁴ Department of Physics and Astronomy, University of Exeter, Stocker Road, Exeter EX4 4QL, UK
⁵ Department of Physics & Namur Institute of Structured Matter (NISM), University of Namur, Rue de Bruxelles 61, 5000 Namur, Belgium
⁶ Micro- and Nanophotonic Materials Group, University of Mons, Place du Parc 20, 7000 Mons, Belgium
* Correspondence: sebastien.mouchet@unamur.be (S.R.M.); branko.kolaric@umons.ac.be (B.K.)

Abstract: Nano-optics explores linear and nonlinear phenomena at the nanoscale to advance fundamental knowledge about materials and their interaction with light in the classical and quantum domains in order to develop new photonics-based technologies. In this perspective article, we review recent progress regarding the application of nonlinear optical methods to reveal the links between photonic structures and functions of natural photonic geometries. Furthermore, nonlinear optics offers a way to unveil and exploit the complexity of the natural world for developing new materials and technologies for the generation, detection, manipulation, and storage of light at the nanoscale, as well as sensing, metrology, and communication.

Keywords: natural photonics; photonics; linear and nonlinear spectroscopy; fluorescence; fluorescence spectroscopy; two-photon fluorescence; second-harmonic generation; third-harmonic generation



Citation: Mara, D.; Bokic, B.; Verbiest, T.; Mouchet, S.R.; Kolaric, B.

Revealing the Wonder of Natural Photonics by Nonlinear Optics. *Biomimetics* **2022**, *7*, 153. <https://doi.org/10.3390/biomimetics7040153>

Academic Editors: Silvia Vignolini, Rox Middleton and Stanislav N. Gorb

Received: 28 July 2022

Accepted: 30 September 2022

Published: 5 October 2022

Publisher's Note: MDPI stays neutral with regard to jurisdictional claims in published maps and institutional affiliations.



Copyright: © 2022 by the authors. Licensee MDPI, Basel, Switzerland. This article is an open access article distributed under the terms and conditions of the Creative Commons Attribution (CC BY) license (<https://creativecommons.org/licenses/by/4.0/>).

1. Introduction

It has been known for a long time that colors in nature are not designed for beauty but are of the utmost importance for communication. Structural colors belong to a special class of colors that have no chemical origin, but they arise from the interaction of light with structures, such as periodically arranged materials [1,2]. Structural colors are ubiquitous colors among insects, fish, and birds. In addition, they are a main topic of research in fields such as biophotonics and biomimetics. In this perspective article, we demonstrate the interest and impact of nonlinear optical studies of photonic structures. We highlight the benefit of nonlinear optical techniques for revealing the details of structured matter at the nanoscale and its interaction with light. We also emphasize that the control of structural colors is essential for various applications in materials science. After introducing the readers to basic concepts of nonlinear optics and natural photonics, we present different cases of natural photonic structures (sometimes combined with artificial materials) investigated by nonlinear optical techniques.

2. Basics of Nonlinear Optics

Nonlinear optics is a part of optics that studies light propagation in nonlinear media. In such media, the polarization P has a nonlinear response to the electric field E . Such optical behavior usually occurs at a high intensity of light, such as the one generated by a laser.

In the linear regime, when an electromagnetic wave interacts with some materials, e.g., a medium containing electric charges, a dipolar type of interaction appears between the dipoles in the medium and the incident electromagnetic fields at a frequency ω [3]. This

interaction can be described by an induced polarization P_{ind} that is linear with the electric field E of the incident light and acts as the source of radiation:

$$P_{\text{ind}} = \chi^{(1)} E, \quad (1)$$

with $\chi^{(1)}$, the linear susceptibility that is related to the refractive index. The response can be modelled by a classical harmonic oscillator, yielding a linear complex refractive index of the medium that scales with ω [3].

However, in the case of high-intensity incident electromagnetic fields, such as laser light (Figure 1), the harmonic oscillator response is not sufficient anymore to describe the observed phenomena [4–7]. The oscillations become anharmonic, i.e., they do not respond linearly to the incident electromagnetic wave. In the nonlinear regime, the induced polarization P_{ind} is expanded in a Taylor series as a function of the total applied electric field. The induced polarization is then written as [7]:

$$P_{\text{ind}} = P^{(1)} + P^{(2)} + P^{(3)} + \dots = \chi^{(1)} E + \chi^{(2)} EE + \chi^{(3)} EEE + \dots \quad (2)$$

with $P^{(1)}$, the linear part of the induced polarization; $P^{(2)}$, the second-order nonlinear response; and $P^{(3)}$, the third order nonlinear response. $\chi^{(1)}$, $\chi^{(2)}$, and $\chi^{(3)}$ are the linear, the first nonlinear, and the second nonlinear susceptibilities, respectively. The latter two quantify the second-order and third-order nonlinear optical response. Since all susceptibilities are related to the refractive index, a nonlinear complex refractive index is obtained.

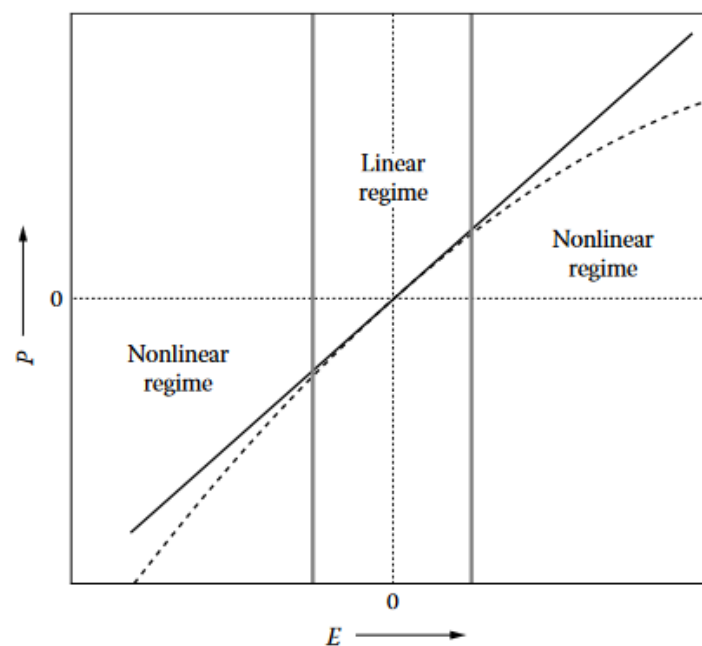


Figure 1. Depending on the intensity of the incident electric field (E), the electric polarization (P) will respond linearly or nonlinearly. As long as the intensity of the electric field is small, the electric polarization is linear to the electric field intensity. This case corresponds to the linear regime. When the intensity of the electric field is high, P is not proportional to E and the regime is nonlinear. Reproduced from Verbiest, T., Clays, K., and Rodriguez, V., 2009. Second-order Nonlinear Optical Characterization Techniques: An Introduction, with permission from Taylor and Francis Group, LLC, a division of Informa plc.

One of the advantages of nonlinear optical techniques is due to the nature of the nonlinear susceptibilities, which are tensors of third and fourth rank, respectively. Especially, second-order nonlinear optical effects, which are described by the third-rank tensor $\chi^{(2)}$, have extremely interesting symmetry properties. In general, $\chi^{(2)}$ is a third-rank tensor with 27 components, but the number of independent and nonvanishing components is

dependent on the symmetry of the medium. All of the components of $\chi^{(2)}$ will vanish in a medium with inversion symmetry. On the other hand, any surface where the symmetry is necessarily broken will typically yield four independent susceptibility components [7]. Since the nonlinear susceptibility directly determines the magnitude and phase of the nonlinear response, the measured response can serve as a means to evaluate the symmetry of the sample.

In addition to the optical properties of matter that can be probed by linear techniques, much more information is available by exploiting the interaction of matter with higher-intensity laser beams. Multiphoton (including two-photon) excitation fluorescence is certainly the most used nonlinear optical technique. In the case of two-photon excitation fluorescence (TPEF), high-intensity photons illuminate a sample [7]. Because of this high intensity, two photons simultaneously interact with the sample, following different selection rules from the photons in the linear light–matter interaction regime. Since two photons are absorbed initially and give rise to only one emitted photon, the resulting photon has a higher energy than each of the two absorbed photons. Multiphoton absorption and fluorescence originate from a third-order nonlinear optical response [7].

In second harmonic generation (SHG), the material also interacts with two photons [7]. Unlike two-photon excitation fluorescence, a third photon is instantaneously emitted (within ca 10^{-15} s) with exactly twice the energy (and, thus, half the wavelength) of the two initial photons. Since SHG is a second-order nonlinear optical process, selection rules that are different from TPEF apply: symmetry requirements such as non-centrosymmetric samples are essential to observe SHG [4–7]. Similarly, third harmonic generation (THG) corresponds to the instantaneous emission of a single photon following the interaction of three incident photons [7]. The generated photon has three times the energy and a third of the wavelength of the three initial photons.

There are multiple advantages to nonlinear techniques with respect to linear optical techniques [8,9]. An important feature is the increase in imaging depth, which can be attributed to multiple factors: first, there is a low probability of multiple photons interacting simultaneously, resulting in a minimal imaging volume at the femtoliter scale by reducing out-of-focus fluorescence. It is therefore possible to image accurately at different depths, similarly to confocal microscopes, and to create 3D reconstructions of the investigated material without the use of a pinhole. Due to the absence of a pinhole, more light can be collected and thus a clearer image can be formed. This also results in an increase in the practical resolution as the pinhole of confocal microscopes is often opened to increase the amount of incoming light to image fluorescing samples. This results in a lower resolution. Practically, the resolution of a multiphoton microscope was shown to approach 250 nm, which equals the best possible resolution of the confocal fluorescence microscopy. Another significant advantage of nonlinear optical techniques is the use of near-infrared excitation light with wavelengths corresponding to the transparency window of biological tissue. This leads to an increase in penetration depth, and it is therefore possible to image sensitive samples without damaging the structure or with minimal damage. Furthermore, most multi-photon microscopes use femtosecond-lasers as an excitation source, which further reduces the risk of photodamage. In addition, no sample preparation is necessary. This constitutes the main advantage over more complicated microscopy techniques such as scanning electron microscopy (SEM) or transmission electron microscopy (TEM) [10,11]. Finally, another interesting application of multiphoton microscopy is the imaging of the local polarization anisotropy via SHG, enabling the user to separately determine the orientation and degree of organization of each non-centrosymmetric component within a sample.

3. Introduction to Natural Photonics

Colours in nature originate from chemical or physical properties of matter, light sources, or combinations of them [1,2]. Chemical colours are caused by pigments. These molecules selectively absorb incident light within a given wavelength band. Examples are eumelanins and pheomelanins, which give rise to brown/black and yellow/red human

skins, respectively [12,13]. Light that is not absorbed by pigments is scattered, giving rise to colours that an observer may perceive. Physical colours are due to interference between incident light and a physical structure. Hence, they are often called structural colours, as a synonym. Structures giving rise to such colours have geometrical dimensions at the micro- or nanoscale. They encompass optical thin films [14–17], diffraction gratings [18–20], Bragg mirrors [21–26], chirped multilayer reflectors [27,28], and photonic crystals [29–34], as well as quasi-ordered [35–40] and randomly disordered [41–44] photonic structures.

Natural photonics is the field of research that studies the interaction between light and such physical structures in nature. Natural structural colours occur in organisms ranging from mammals such as primates (including human blue eyes) and marsupials, fish, or birds such as hummingbirds and pigeons to insects such as butterflies and beetles (Figure 2) [1,2,45].

This section introduces key concepts and presents some selected case studies from natural photonics, in the linear regime.

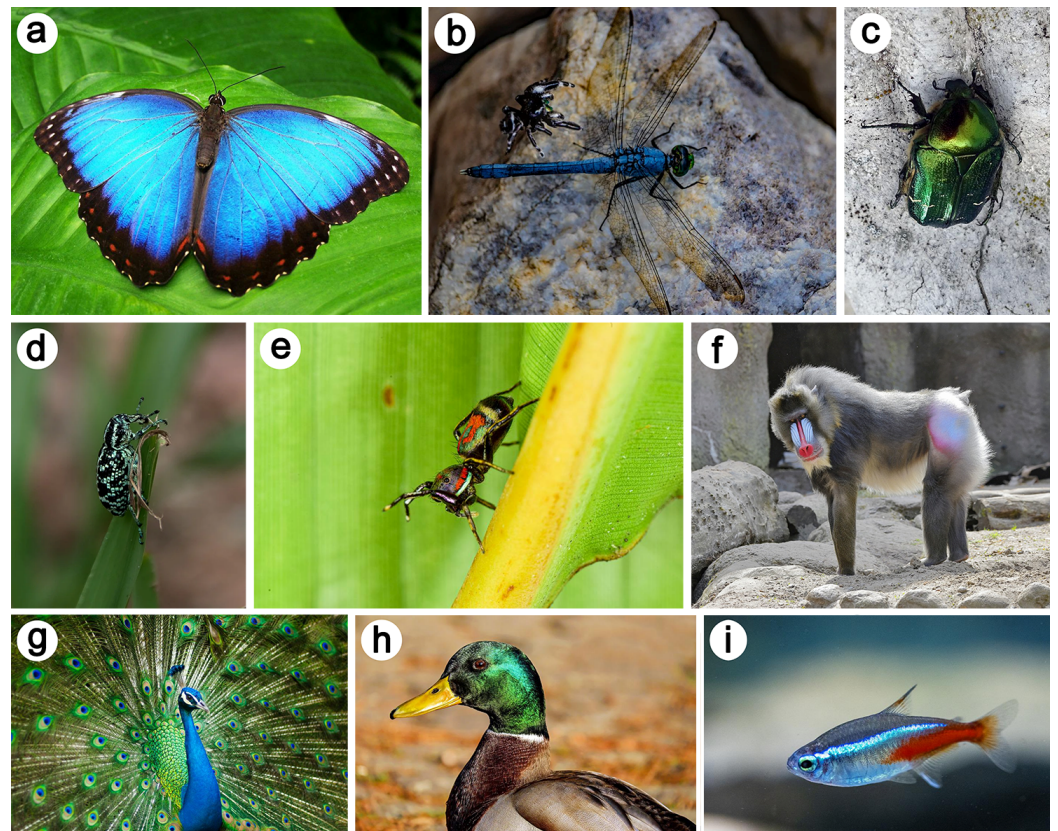


Figure 2. Many examples of structural colours are found in the integuments of natural organisms. They include the wings of the common morpho *Morpho peleides* (a), the body of some dragonfly species (b), the thorax and elytra of the green rose chafer *Cetonia aurata* (c), the body of the Botany Bay diamond weevil *Chrysolopus spectabilis* (d), the integuments of some jumping spider species (e), the skin of the mandrill *Mandrillus sphinx* (f), the feathers of the Indian peafowl *Pavo cristatus* (g), the head of the mallard *Anas platyrhynchos* (h), and the body of the neon tetra fish *Paracheirodon innesi* (i). Reproduced from from <https://pixabay.com/> accessed on 27 July 2022.

One striking example is the case of the male beetle *Hoplia coerulea* (Figure 3). The blue-violet iridescent colour of its elytra and body observed in reflection with incident visible light arises from a photonic structure, namely, a porous periodic multilayer, within the round scales occurring on its body [46,47].

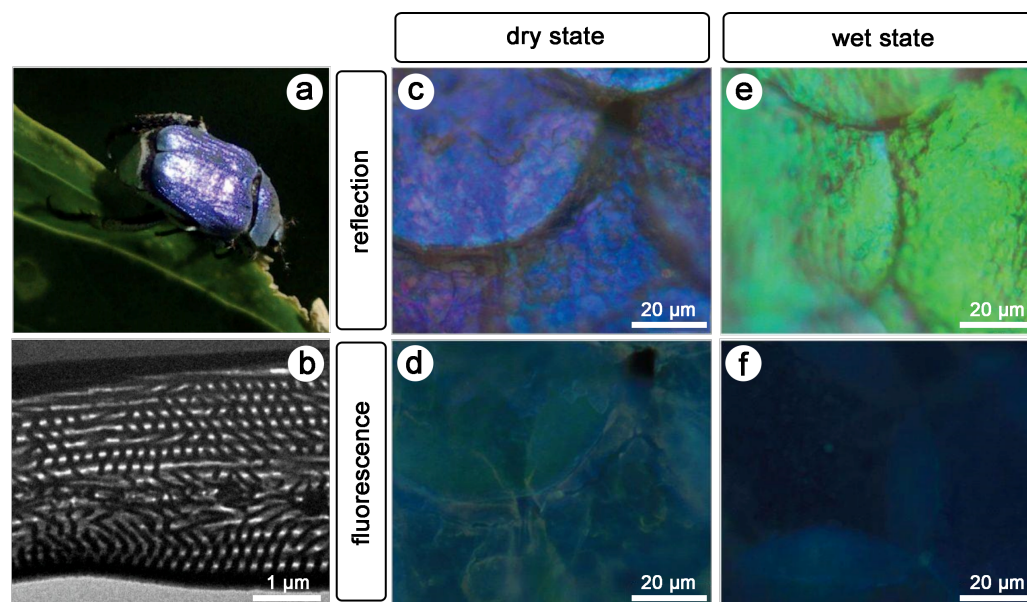


Figure 3. The blue-violet colour of the male beetle *Hoplia coerulea* (a) originates from a multilayer photonic structure. This porous periodic multilayer (b) occurs in the scales covering the elytra (c) and body of the insect. Upon UV light illumination, the scales display a turquoise colour through fluorescence (d). When in contact with water, the scales turn to green (e) and navy blue (f) under visible and UV light illumination, respectively. Reproduced from Mouchet, S.R., Lobet, M., Kolaric, B., Kaczmarek, A.M., Van Deun, R., Vukusic, P., Deparis, O., and Van Hooijdonk, E., 2016. Controlled fluorescence in a beetle’s photonic structure and its sensitivity to environmentally induced changes. *Proc. R. Soc. B* 283, 20162334, with permission from The Royal Society.

This multilayer is mainly composed of chitin, the building material of insects [1,2]. Upon contact with liquids and vapour, these scales change their colour to green [48–52]: the spectral reflectance peak red-shifts. This colour change arises from the penetration of some liquid into the pores of the scales, filling the pores and changing the refractive index.

Furthermore, one-photon excitation fluorescence (OPEF) emission was observed when the beetle was illuminated with UV light (Figure 3d) [53,54]. The colour of the scales covering the elytra and body of this insect is turquoise. This phenomenon arises in biological organisms, the integuments of which contain so-called fluorophores [55,56]. Examples include birds [44,57–59], insects [60–71], arachnids [72,73], mammals [74], amphibians [75,76], reptiles [77], marine animals [78,79], and plants [80,81] (Figure 2). These molecules emit longer-wavelength light (typically, visible photons) following the absorption of incident shorter-wavelength light (typically, UV, violet or blue photons).

Fluorescence emission results from transition between two real electron states with the same multiplicity of spin. The role, if any, of fluorescence (Figure 4) in visual communication is unclear [55,56]. Biopterin, the green fluorescent protein (GFP), papiliochrom II, psittacofulvin, and resilin are examples of fluorophores.

When light emission takes place in photonic structures, the structure may modify the directionality, the decay time, and the spectral intensity of the emitted light [82,83]. Light emission can be reduced or even inhibited if the emission wavelength is in the range of the photonic bandgap of the structure. The decay time of the excited is then increased and can, theoretically, be infinite. When such light emitted in a photonic structure originates from fluorescence, this phenomenon is often referred to as controlled fluorescence. The confinement of fluorophores in natural photonic structures was found in several species [84–88], including the male beetle *H. coerulea* [53,54]. Upon contact with water, the peak in the fluorescence emission spectrum from the scales of this beetle blue-shifts, giving rise to a navy blue colour (Figure 3d,f). Following the penetration of the porous structure by water, the local density of optical states (LDOS) is modified, leading to the observed colour change.

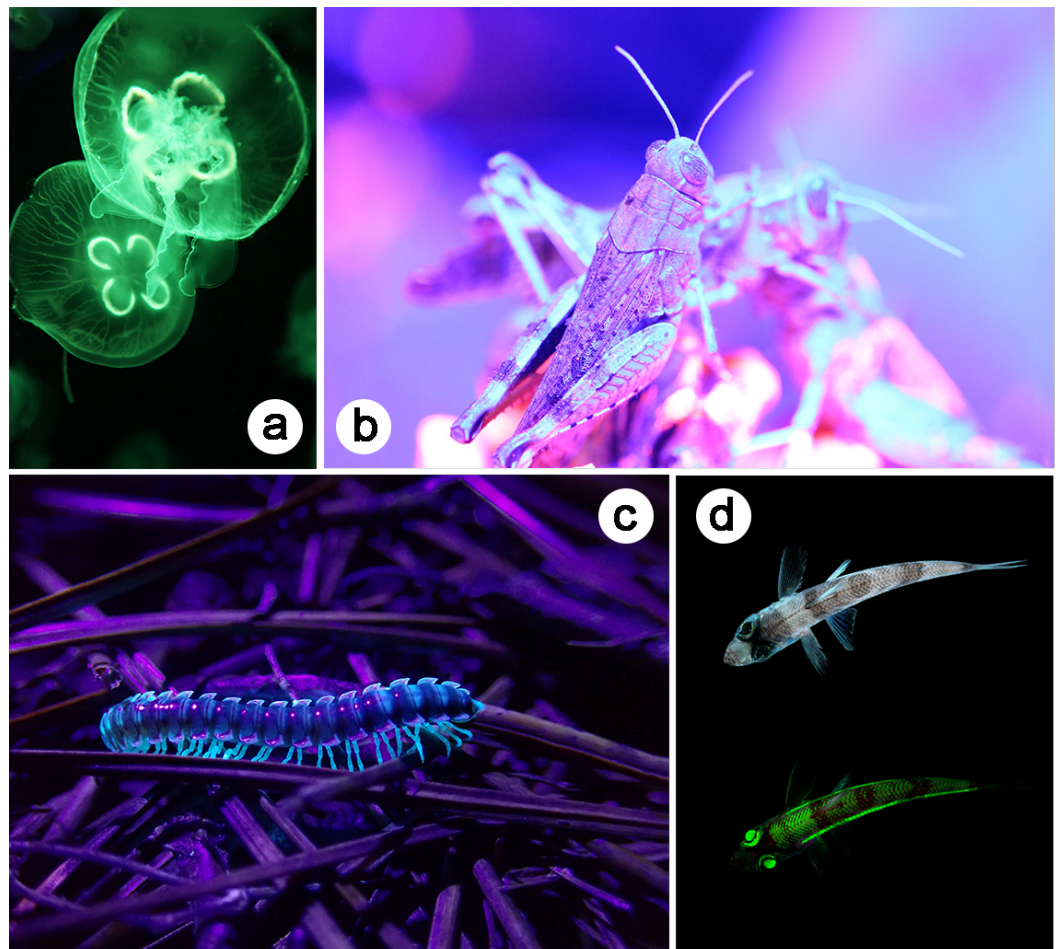


Figure 4. Fluorescence is ubiquitous in the integuments of natural organisms. The integuments of some jellyfish species (a), some grasshopper species (b), some millipede species (c), and some greeneye fish species (d) are known for their fluorescent properties. (d) Top (bottom): greeneye fish under visible (UV) light. Reproduced from from pixabay.com.

The interaction between fluorescent light and photonic structures was also highlighted in the scales covering the elytra of longhorn beetles *Celosterna pollinosa sulfurea* and *Phosphorus virescens* [68]. These scales exhibit yellow and turquoise colours under visible and UV incident light, respectively, with an underlying basal brown membrane (Figure 5a–d), akin to the beetles *Euchroea auripigmenta* and *Trictenotoma childreni* [69,70]. Through scatterograms and detailed series of simulations, it was demonstrated that the scales play the role of waveguides for light emitted by the embedded fluorophores (Figure 5e,f).

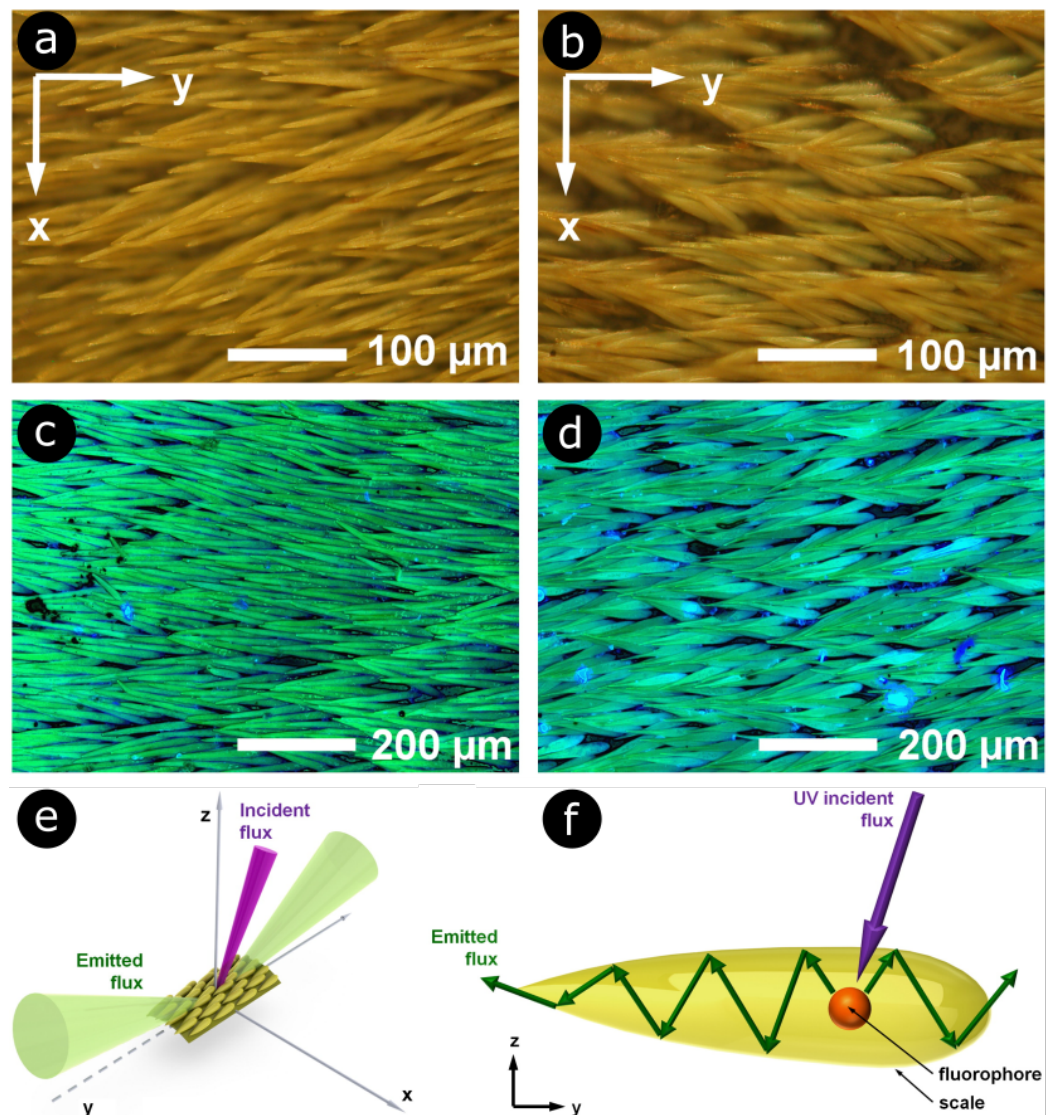


Figure 5. The elytra of longhorn beetles *Celosterna pollinosa sulfurea* and *Phosphorus virescens* are covered by elongated scales, in which fluorophores are embedded. These scales act as waveguides for the light emitted by the fluorophores. They display a yellow colour under visible light for *C. pollinosa sulfurea* (a) and *P. virescens* (b) (here, observation by optical microscopy). Under UV light, the observed colour is turquoise in both respective cases (c,d). Upon illumination with UV light (represented in magenta), embedded fluorophores mostly emitted within two emission cones (in green) (e) due to a waveguide effect taking place within the scales (f). Reproduced from Van Hooijdonk, E., Barthou, C., Vigneron, J.-P., and Berthier, S., 2013. Yellow structurally modified fluorescence in the longhorn beetles *Celosterna pollinosa sulfurea* and *Phosphorus virescens* (Cerambycidae). *J. Lumin.* 136, 313–321, with permission from Elsevier.

4. Nonlinear Optical Study of Natural Photonic Structures

Harnessing light–matter interaction in a nonlinear regime, researchers and engineers developed various tools for imaging and spectroscopy analyses of biological samples [8,62,89–105]. Nonlinear optical imaging and spectroscopy have proved to be versatile and efficient techniques in biomedical and biological research, with many benefits, including an increase in analytic depth and a reduction in photodamage, with respect to classical linear optical techniques [8]. In general, nonlinear optical studies led to a better understanding of the link between the optical response and geometries of natural photonic structures that are essential for potential applications of these structures in biomimetics and quantum technology [9].

For instance, the multi-excited states character of the fluorophores embedded in the integuments of *H. coerulea* were revealed by comparing OPEF spectra with TPEF measurements [106] (Figure 6a–d).

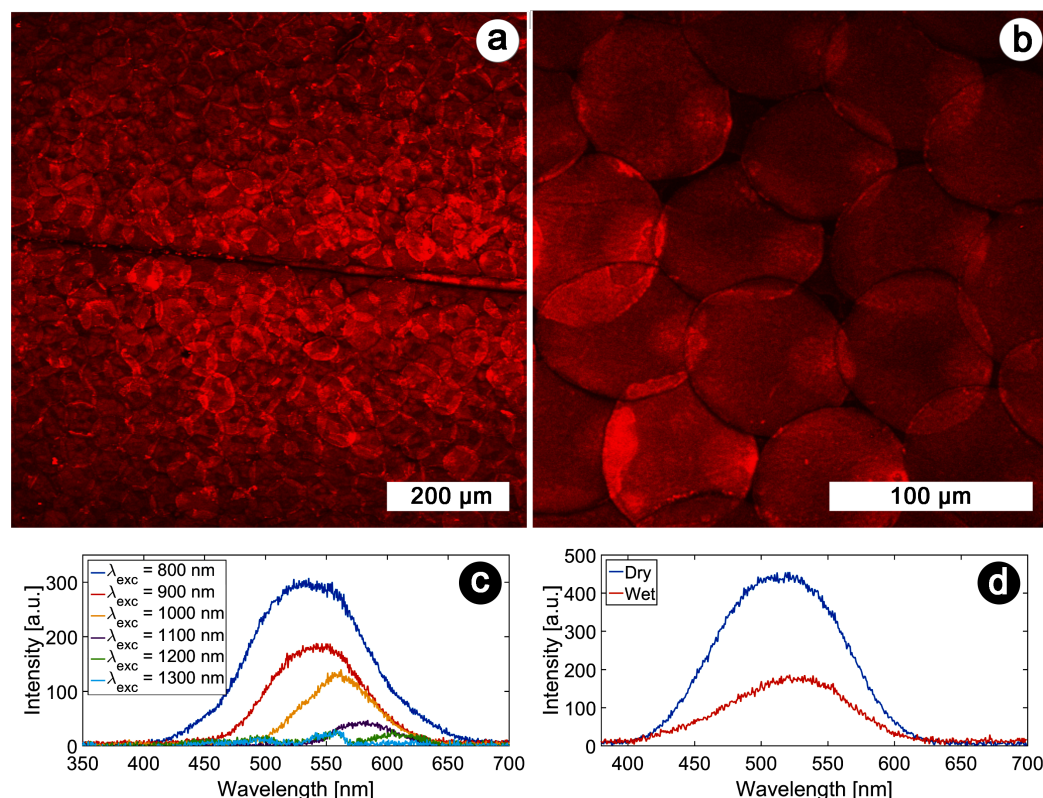


Figure 6. TPEF microscopy and spectroscopy of the scales covering *H. coerulea*'s elytra. An intense TPEF response was detected from the elytra of the male beetle *H. coerulea* with an excitation wavelength equal to 900 nm (a) and 800 nm (b). TPEF excitation spectra were measured with various excitation wavelengths (c). Upon contact with water (d), the emitted intensity decreases and the peak wavelength red-shifts slightly (the excitation wavelength equals 800 nm). Scale bars: (a) 200 μm and (b) 100 μm . Reproduced from Mouchet, S. R., Verstraete, C., Mara, D., Van Cleuvenbergen, S., Finlayson, E. D., Van Deun, R., Deparis, O., Verbiest, T., Maes, B., Vukusic, P., and Kolaric, B., 2019 Nonlinear optical spectroscopy and two-photon excited fluorescence spectroscopy reveal the excited states of fluorophores embedded in a beetle's elytra, *Interface Focus* 9(1), 20180052, with permission from The Royal Society.

This provided insight into the electron structure of the embedded fluorophores.

Furthermore, local-form anisotropy arising from local-direction-dependent subwavelength morphology was shown to influence both linear and nonlinear optical responses (in reflection and emission) thanks to THG spectroscopy [106]. The anisotropy is caused due to the subwavelength spacers located in the mixed air-chitin layers (Figure 3b). These spacers are locally parallel.

This finding highlighted the need to take a more accurate model into account for predicting some of the optical properties of the elytra of this beetle.

Similarly, the yellow and fluorescent elongated scales covering the elytra of the log-boring beetle *Trictenotoma childreni* were investigated by nonlinear optical methods, including OPEF, TPEF, and SHG microscopy and spectroscopy (Figure 7) [70]. These scales appear similar to the ones of the longhorn beetles *Celosterna pollinosa sulfurea* and *Phosphorus virescens* (Figure 5) [68]. They contain fluorophores that give rise to a yellow visual appearance upon UV illumination. These observations allowed one to highlight the non-centrosymmetric nature of the fluorophores embedded within these scales [70].

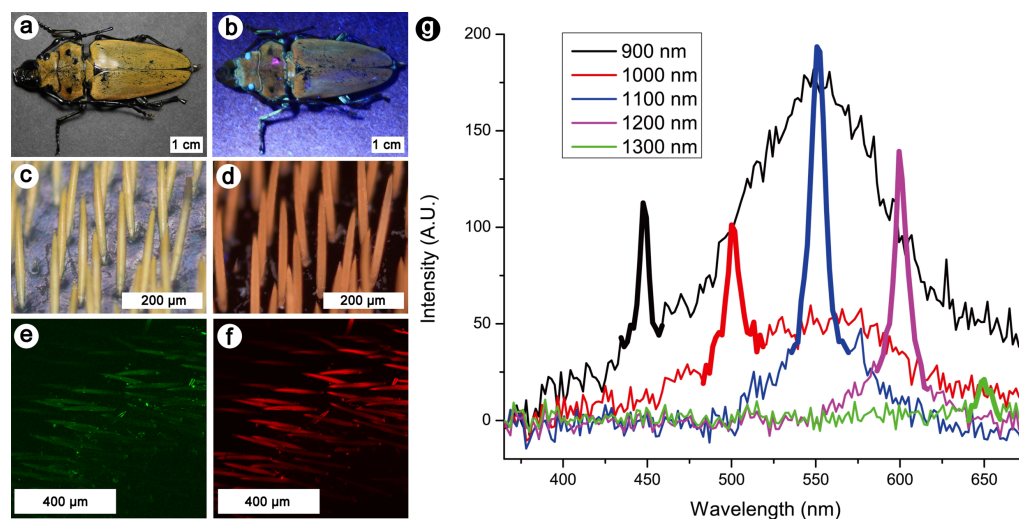


Figure 7. The yellow and fluorescent scales occurring on the elytra of the log-boring beetle *T. childreni* were investigated by nonlinear optical techniques, including OPEF, TPEF, and SHG microscopy and spectroscopy. The elytra exhibit a yellow colour under both incident visible white (a) and UV (b) light. This colour is due to the presence of elongated scales covering the elytra (c,d). Under visible (c) or UV light (d), they appear in shades of yellow. Upon excitation with a fundamental wavelength of 1000 nm, a SHG (e) and a TPEF (f) signal can be detected from the scales (here observed by microscopy in false colours). Multiphoton emission spectra of the log-boring beetle's scales measured with various excitation wavelengths (g) exhibit SHG peaks at half the excitation wavelengths (thick lines). TPEF peaks were observed around 550 nm at most excitation wavelengths. Reproduced from Mouchet, S. R., Verstraete, C., Kaczmarek, A. M., Mara, D., van Cleuvenbergen, S., Van Deun, R., Verbiest, T., Maes, B., Vukusic, P., and Kolaric, B., 2019, Unveiling the nonlinear optical response of *Trictenotoma childreni* longhorn beetle, *J. Biophot.* 12(9), 12:e201800470, with permission from John Wiley and Sons.

So far, various natural photonic structures from different insects, including butterflies and cicadas, have been investigated for sensing and materials-oriented applications. For example, corrugated natural photonic structures offer a unique possibility to develop new sensing platforms by combing corrugation at different scales, plasmonic properties, and surface-enhanced Raman spectroscopy (SERS) [107–111]. The work of Garrett and coworkers clearly shows the benefit of natural and bioinspired structuring, which can be used for different sensing applications (Figure 8) [108–110]. The development of such novel platforms relying on SERS will lead to the fast and accurate screening of chemical, biochemical, and pharmaceutical compounds, which is crucial for the growing fields of proteomics, genomics, molecular medicine, and biophysics, as well as for the development of assays for the detection of diseases [107,112].

The work of Stoddart and coworkers highlighted that practical applications of SERS for sensing depend on the development of manufacturing methods that will be used to mimic the complex morphology of insect integuments [107]. It pointed out the importance of biomimetics for the advancement of materials science [107]. In addition, it was shown that the enhancement of SERS also depends on the aspect ratio of metallic nanoparticles. The presence of different multiscale groove-like structures presented the possibility of developing smart surfaces for controlling optical response and wetting properties [113]. Structuring materials have a significant effect on the latter, as was demonstrated both theoretically and experimentally, specifically at different length scales [114–116].

Furthermore, the natural photonic structures occurring in the wings of the butterfly *Cymothoe sangaris* were used for tuning the upconversion luminescence of nanoparticles doped with lanthanide ($\text{NaYF}_4 : \text{Yb}^{3+}, \text{Er}^{3+}$) [117]. Upon illumination with a light at 980 nm, both red and green emission bands of $\text{NaYF}_4 : \text{Yb}^{3+}, \text{Er}^{3+}$ could be controlled, producing different luminescent colours Figure 9. Doping natural photonic structures with

materials including metals and oxides also presents the possibility of using these structures as templates to design nanocorrugated materials (with complex shapes and geometries) on demand for various material applications [118].

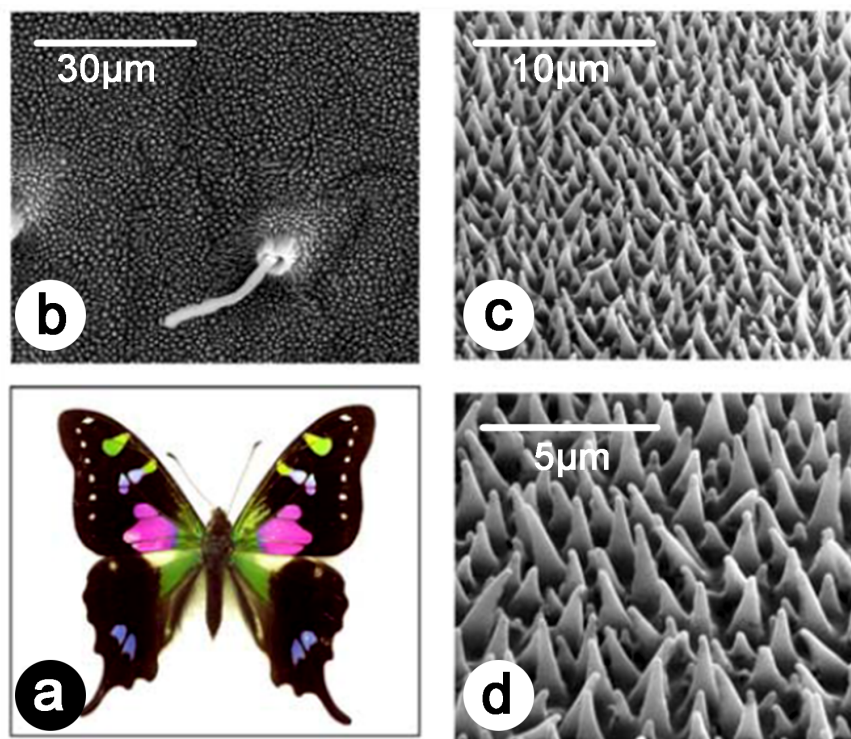


Figure 8. The structures occurring on the wings of the purple spotted swallowtail butterfly (*Graphium weiskei*) coated with a metal thin film were found to be an excellent substrate for SERS, in terms of biocompatibility and sensitivity [108–110]. *G. weiskei* (a) exhibit conical microstructures on its wings (b–d) as observed here by SEM. After coating by gold or silver, these structures can be used to detect protein binding from direct observation of the modifications in the SERS response. Reproduced from Garrett, N. L., Vukusic, P., Ogrin, F., Sirotkin, E., Winlove, C. P., and Moger, J., 2009, Spectroscopy on the wing: Naturally inspired SERS substrates for biochemical analysis, *J. Biophot.* 2(3), 157–166.

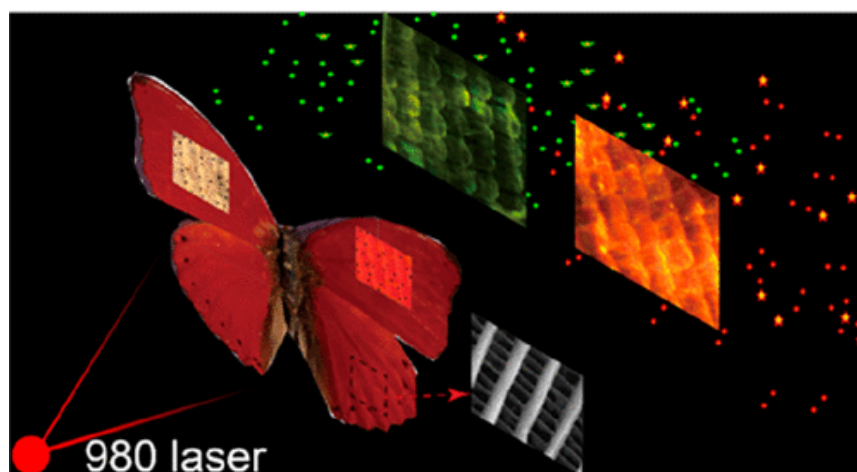


Figure 9. The upconversion luminescence of nanoparticles doped with lanthanide ($\text{NaYF}_4 : \text{Yb}^{3+}, \text{Er}^{3+}$) was controlled thanks to the natural photonic crystals occurring in the wings of the butterfly *Cymothoe sangaris*. With a 980 nm incident light, various luminescent colours were generated. Reproduced from Gao, T., Zhu, X., Wu, X. J., Zhang, B., and Liu, H. L., 2021, Selectively Manipulating Upconversion Emission Channels with Tunable Biological Photonic Crystals, *J. Phys. Chem. C*, 125(1), 732–739, with permission from ACS Publications.

5. Conclusions

In this perspective article, we presented theoretical key concepts of nonlinear optics and discussed the results of nonlinear optical studies in the field of natural photonics. Because nonlinear optical techniques are inherently sensitive to symmetry; the presence of interfaces; and chirality, they offer a more detailed insight into the molecular properties of biomaterials. This is crucial for applications in different areas of material science. Even though, at the moment, nonlinear optical investigations of natural photonics are still at their infant stage of development, the primary aim of this article is to draw the attention of the broad material, photonic, and biological scientific communities to the capability of nonlinear optics, which could be used to forge new horizons in physical, biological and material research.

Author Contributions: Conceptualization, B.K. and S.R.M.; writing—original draft: S.R.M. and B.K.; and writing—review & editing: all authors. All authors have read and agreed to the published version of the manuscript.

Funding: DM acknowledges KU Leuven Postdoctoral Mandate Internal Funds (PDM) for a Postdoctoral fellowship (PDM/20/092). BB and BK acknowledge financial support of the Ministry of Education, Science, and Technological Development of the Republic of Serbia (grant III 45016). BB, BK, and DM acknowledge the support of the Office of Naval Research Global through the Research Grant N62902-22-1-2024. SRM was supported by a BEWARE Fellowship (Convention n°2110034) of the Walloon Region (Marie Skłodowska-Curie Actions of the European Union #847587), as a Postdoctoral Researcher. TV acknowledges financial support from the Hercules Foundation. BK acknowledges support from the Belgian National Fund for Scientific Research (FRS-FNRS).

Conflicts of Interest: The authors declare no conflict of interest. The funders had no role in the design of the study; in the collection, analyses, or interpretation of data; in the writing of the manuscript; or in the decision to publish the results.

References

1. Kinoshita, S. *Structural Colors in the Realm of Nature*; World Scientific Publishing Co.: Singapore, 2008.
2. Mouchet, S.R.; Deparis, O. *Natural Photonics and Bioinspiration*; Artech House: Boston, MA, USA, 2021.
3. Hecht, E. *Optics*; Addison-Wesley Publishing Company: Reading, MA, USA, 2001.
4. Stratton, J. *Electromagnetic Theory*; McGraw-Hill: New York, NY, USA, 1941.
5. Böttcher, C. *Theory of Electric Polarization*, 2nd ed.; Elsevier: Amsterdam, The Netherlands, 1973.
6. Zernike, F.; Midwinter, J. *Applied Nonlinear Optics*; Wiley: New York, NY, USA, 1973.
7. Verbiest, T.; Clays, K.; Rodriguez, V. *Second-Order Nonlinear Optical Characterization Techniques: An Introduction*; CRC Press Taylor & Francis Group: Boca Raton, FL, USA, 2009.
8. Zipfel, W.R.; Williams, R.M.; Webb, W.W. Nonlinear magic: Multiphoton microscopy in the biosciences. *Nat. Biotechnol.* **2003**, *21*, 1369. [[CrossRef](#)] [[PubMed](#)]
9. Verstraete, C.; Mouchet, S.R.; Verbiest, T.; Kolaric, B. Linear and nonlinear optical effects in biophotonic structures using classical and nonclassical light. *J. Biophotonics* **2019**, *12*, e201800262. [[CrossRef](#)]
10. Pathan, A.; Bond, J.; Gaskin, R. Sample preparation for scanning electron microscopy of plant surfaces—Horses for courses. *Micron* **2008**, *39*, 1049–1061. [[CrossRef](#)] [[PubMed](#)]
11. Ayache, J.; Beaunier, L.; Boumendil, J.; Ehret, G.; Laub, D. *Sample Preparation Handbook for Transmission Electron Microscopy*; Springer: New York, NY, USA, 2010.
12. Slominski, A.; Tobin, D.J.; Shibahara, S.; Wortsman, J. Melanin Pigmentation in Mammalian Skin and Its Hormonal Regulation. *Physiol. Rev.* **2004**, *84*, 1155–1228. [[CrossRef](#)]
13. Ito, S.; Wakamatsu, K. Diversity of human hair pigmentation as studied by chemical analysis of eumelanin and pheomelanin. *J. Eur. Acad. Dermatol. Venereol.* **2011**, *25*, 1369–1380. [[CrossRef](#)] [[PubMed](#)]
14. Stavenga, D.G.; Giraldo, M.A.; Leertouwer, H.L. Butterfly wing colors: Glass scales of *Graphium sarpedon* cause polarized iridescence and enhance blue/green pigment coloration of the wing membrane. *J. Exp. Biol.* **2010**, *213*, 1731–1739. [[CrossRef](#)]
15. Stavenga, D.G.; Matsushita, A.; Arikawa, K.; Leertouwer, H.L.; Wilts, B.D. Glass scales on the wing of the swordtail butterfly *Graphium sarpedon* act as thin film polarizing reflectors. *J. Exp. Biol.* **2012**, *215*, 657–662. [[CrossRef](#)]
16. Stavenga, D. Thin film and multilayer optics cause structural colors of many insects and birds. *Mater. Today Proc.* **2014**, *1S*, 109–121. [[CrossRef](#)]
17. Siddique, R.; Vignolini, S.; Bartels, C.; Wacker, I.; Hölscher, H. Colour formation on the wings of the butterfly *Hypolimnas salmacis* Scale Stacking. *Sci. Rep.* **2016**, *6*, 36204. [[CrossRef](#)]

18. Vukusic, P.; Sambles, J.R.; Lawrence, C.R.; Wootton, R.J. Limited-view iridescence in the butterfly *Ancyluris Meliboeus*. *Proc. R. Soc. Lond. Ser. B Biol. Sci.* **2002**, *269*, 7–14. [[CrossRef](#)]
19. Vukusic, P.; Kelly, R.; Hooper, I. A biological sub-micron thickness optical broadband reflector characterized using both light and microwaves. *J. R. Soc. Interface* **2009**, *6*, S193–S201. [[CrossRef](#)] [[PubMed](#)]
20. Vigneron, J.P.; Simonis, P.; Aiello, A.; Bay, A.; Windsor, D.M.; Colomer, J.F.; Rassart, M. Reverse color sequence in the diffraction of white light by the wing of the male butterfly *Pierella Luna* (Nymphalidae: Satyrinae). *Phys. Rev. E* **2010**, *82*, 021903. [[CrossRef](#)] [[PubMed](#)]
21. Biró, L.P.; Bálint, Z.; Kertész, K.; Vértesy, Z.; Márk, G.I.; Horváth, Z.E.; Balázs, J.; Méhn, D.; Kiricsi, I.; Lousse, V.; et al. Role of photonic-crystal-type structures in the thermal regulation of a Lycaenid butterfly sister species pair. *Phys. Rev. E* **2003**, *67*, 021907. [[CrossRef](#)] [[PubMed](#)]
22. Yoshioka, S.; Kinoshita, S. Single-scale spectroscopy of structurally colored butterflies: measurements of quantified reflectance and transmittance. *J. Opt. Soc. Am. A* **2006**, *23*, 134–141. [[CrossRef](#)] [[PubMed](#)]
23. Noyes, J.A.; Vukusic, P.; Hooper, I.R. Experimental method for reliably establishing the refractive index of buprestid beetle exocuticle. *Opt. Express* **2007**, *15*, 4351–4358. [[CrossRef](#)] [[PubMed](#)]
24. Kertész, K.; Molnár, G.; Vértesy, Z.; Koós, A.; Horváth, Z.; Márk, G.; Tapasztó, L.; Bálint, Z.; Tamáska, I.; Deparis, O.; et al. Photonic band gap materials in butterfly scales: A possible source of “blueprints”. E-MRS 2007 Spring Conference Symposium A: Sub-wavelength photonics throughout the spectrum: Materials and Techniques. *Mater. Sci. Eng. B* **2008**, *149*, 259–265. [[CrossRef](#)]
25. Wilts, B.D.; Leertouwer, H.L.; Stavenga, D.G. Imaging scatterometry and microspectrophotometry of lycaenid butterfly wing scales with perforated multilayers. *J. R. Soc. Interface* **2009**, *6*, S185–S192. [[CrossRef](#)] [[PubMed](#)]
26. Stavenga, D.G.; Wilts, B.D.; Leertouwer, H.L.; Hariyama, T. Polarized iridescence of the multilayered elytra of the Japanese jewel beetle, *Chrysochroa Fulgidissima*. *Philos. Trans. R. Soc. B Biol. Sci.* **2011**, *366*, 709–723. [[CrossRef](#)]
27. Vigneron, J.P.; Pasteels, J.M.; Windsor, D.M.; Vértesy, Z.; Rassart, M.; Seldrum, T.; Dumont, J.; Deparis, O.; Lousse, V.; Biró, L.P.; et al. Switchable reflector in the Panamanian tortoise beetle *Charidotella Egregia* (Chrysomelidae: Cassidinae). *Phys. Rev. E* **2007**, *76*, 031907. [[CrossRef](#)]
28. Pasteels, J.M.; Deparis, O.; Mouchet, S.R.; Windsor, D.M.; Billen, J. Structural and physical evidence for an endocuticular gold reflector in the tortoise beetle, *Charidotella Ambita*. *Arthropod Struct. Dev.* **2016**, *45*, 509–518. [[CrossRef](#)]
29. Kertész, K.; Bálint, Z.; Vértesy, Z.; Márk, G.I.; Lousse, V.; Vigneron, J.P.; Rassart, M.; Biró, L.P. Gleaming and dull surface textures from photonic-crystal-type nanostructures in the butterfly *Cyanophrys remus*. *Phys. Rev. E* **2006**, *74*, 021922. [[CrossRef](#)] [[PubMed](#)]
30. Michielsen, K.; Stavenga, D. Gyroid cuticular structures in butterfly wing scales: Biological photonic crystals. *J. R. Soc. Interface* **2008**, *5*, 85–94. [[CrossRef](#)] [[PubMed](#)]
31. Saranathan, V.; Osuji, C.O.; Mochrie, S.G.J.; Noh, H.; Narayanan, S.; Sandy, A.; Dufresne, E.R.; Prum, R.O. Structure, function, and self-assembly of single network gyroid (I4₁32) Photonic Cryst. Butterfly Wing Scales. *Proc. Natl. Acad. Sci. USA* **2010**, *107*, 11676–11681. [[CrossRef](#)] [[PubMed](#)]
32. Pouya, C.; Vukusic, P. Electromagnetic characterization of millimetre-scale replicas of the gyroid photonic crystal found in the butterfly *Parides Sesostris*. *Interface Focus* **2012**, *2*, 645–650. [[CrossRef](#)]
33. Mouchet, S.R.; Vigneron, J.P.; Colomer, J.F.; Vandembem, C.; Deparis, O. Additive photonic colors in the Brazilian diamond weevil: *Entimus imperialis*. *Proc. SPIE* **2012**, *8480*, 848003. [[CrossRef](#)]
34. Mouchet, S.; Colomer, J.F.; Vandembem, C.; Deparis, O.; Vigneron, J.P. Method for modeling additive color effect in photonic polycrystals with form anisotropic elements: The case of *Entimus Imp. Weevil*. *Opt. Express* **2013**, *21*, 13228–13240. [[CrossRef](#)]
35. Prum, R.O.; Torres, R.H.; Williamson, S.W.; Dyck, J. Coherent light scattering by blue feather barbs. *Nature* **1998**, *396*, 28–29. [[CrossRef](#)]
36. Prum, R.O.; Torres, R.H. A Fourier Tool for the Analysis of Coherent Light Scattering by Bio-Optical Nanostructures1. *Integr. Comp. Biol.* **2003**, *43*, 591–602. [[CrossRef](#)]
37. Prum, R.O.; Torres, R. Structural colouration of avian skin: Convergent evolution of coherently scattering dermal collagen arrays. *J. Exp. Biol.* **2003**, *206*, 2409–2429. [[CrossRef](#)]
38. Prum, R.O.; Torres, R.H. Structural colouration of mammalian skin: Convergent evolution of coherently scattering dermal collagen arrays. *J. Exp. Biol.* **2004**, *207*, 2157–2172. [[CrossRef](#)]
39. Henze, M.J.; Lind, O.; Wilts, B.D.; Kelber, A. Pterin-pigmented nanospheres create the colours of the polymorphic damselfly *Ischnura Elegans*. *J. R. Soc. Interface* **2019**, *16*, 20180785. [[CrossRef](#)] [[PubMed](#)]
40. Mouchet, S.R.; Luke, S.; McDonald, L.T.; Vukusic, P. Optical costs and benefits of disorder in biological photonic crystals. *Faraday Discuss.* **2020**, *223*, 9–48. [[CrossRef](#)] [[PubMed](#)]
41. Morehouse, N.L.; Vukusic, P.; Rutowski, R. Pterin pigment granules are responsible for both broadband light scattering and wavelength selective absorption in the wing scales of pierid butterflies. *Proc. R. Soc. B Biol. Sci.* **2007**, *274*, 359–366. [[CrossRef](#)] [[PubMed](#)]
42. Stavenga, D.G.; Stowe, S.; Siebke, K.; Zeil, J.; Arikawa, K. Butterfly wing colours: Scale beads make white pierid wings brighter. *Proc. R. Soc. Lond. Ser. B Biol. Sci.* **2004**, *271*, 1577–1584. [[CrossRef](#)] [[PubMed](#)]
43. Stavenga, D.G.; Giraldo, M.A.; Hoenders, B.J. Reflectance and transmittance of light scattering scales stacked on the wings of pierid butterflies. *Opt. Express* **2006**, *14*, 4880–4890. [[CrossRef](#)]

44. Ladouce, M.; Barakat, T.; Su, B.L.; Deparis, O.; Mouchet, S.R. Scattering of ultraviolet light by avian eggshells. *Faraday Discuss.* **2020**, *223*, 63–80. [[CrossRef](#)]
45. Mouchet, S.R.; Vukusic, P. Structural Colours in Lepidopteran Scales. *Adv. Insect Physiol.* **2018**, *54*, 1–53. [[CrossRef](#)]
46. Vigneron, J.P.; Colomer, J.F.m.; Vigneron, N.; Lousse, V. Natural layer-by-layer photonic structure in the squamae of *Hoplia Coerulea* (Coleoptera). *Phys. Rev. E* **2005**, *72*, 061904. [[CrossRef](#)]
47. Mouchet, S.; Lobet, M.; Kolaric, B.; Kaczmarek, A.; Van Deun, R.; Vukusic, P.; Deparis, O.; Van Hooijdonk, E. Photonic scales of *Hoplia Coerulea* Beetle: Any Colour You Like. *Mater. Today Proc.* **2017**, *4*, 4979–4986. [[CrossRef](#)]
48. Rassart, M.; Simonis, P.; Bay, A.; Deparis, O.; Vigneron, J.P. Scale coloration change following water absorption in the beetle *Hoplia Coerulea* (Coleoptera). *Phys. Rev. E* **2009**, *80*, 031910. [[CrossRef](#)]
49. Mouchet, S.R.; Su, B.L.; Tabarrant, T.; Lucas, S.; Deparis, O. *Hoplia Coerulea*, A Porous Nat. Photonic Struct. Template Opt. Vap. Sensor. *Proc. SPIE* **2014**, *9127*. [[CrossRef](#)]
50. Mouchet, S.R.; Tabarrant, T.; Lucas, S.; Su, B.L.; Vukusic, P.; Deparis, O. Vapor sensing with a natural photonic cell. *Opt. Express* **2016**, *24*, 12267–12280. [[CrossRef](#)] [[PubMed](#)]
51. Mouchet, S.; Van Hooijdonk, E.; Welch, V.; Louette, P.; Colomer, J.F.; Su, B.L.; Deparis, O. Liquid-induced colour change in a beetle: The concept of a photonic cell. *Sci. Rep.* **2016**, *6*, 19322. [[CrossRef](#)] [[PubMed](#)]
52. Mouchet, S.; Van Hooijdonk, E.; Welch, V.; Louette, P.; Tabarrant, T.; Vukusic, P.; Lucas, S.; Colomer, J.F.; Su, B.L.; Deparis, O. Assessment of environmental spectral ellipsometry for characterising fluid-induced colour changes in natural photonic structures. *Mater. Today Proc.* **2017**, *4*, 4987–4997. [[CrossRef](#)]
53. Van Hooijdonk, E.; Berthier, S.; Vigneron, J.P. Bio-inspired approach of the fluorescence emission properties in the scarabaeid beetle *Hoplia Coerulea* (Coleoptera): Model. Transf.-Matrix Opt. Simulations. *J. Appl. Phys.* **2012**, *112*, 114702. [[CrossRef](#)]
54. Mouchet, S.R.; Lobet, M.; Kolaric, B.; Kaczmarek, A.M.; Van Deun, R.; Vukusic, P.; Deparis, O.; Van Hooijdonk, E. Controlled fluorescence in a beetle's photonic structure and its sensitivity to environmentally induced changes. *Proc. R. Soc. Lond. B Biol. Sci.* **2016**, *283*. [[CrossRef](#)]
55. Lagorio, M.G.; Cordon, G.B.; Iriel, A. Reviewing the relevance of fluorescence in biological systems. *Photochem. Photobiol. Sci.* **2015**, *14*, 1538–1559. [[CrossRef](#)]
56. Marshall, J.; Johnsen, S. Fluorescence as a means of colour signal enhancement. *Philos. Trans. R. Soc. Lond. B Biol. Sci.* **2017**, *372*. [[CrossRef](#)]
57. Arnold, K.E.; Owens, I.P.F.; Marshall, N.J. Fluorescent Signaling in Parrots. *Science* **2002**, *295*, 92. [[CrossRef](#)]
58. McGraw, K.J.; Toomey, M.B.; Nolan, P.M.; Morehouse, N.I.; Massaro, M.; Jouventin, P. A description of unique fluorescent yellow pigments in penguin feathers. *Pigment Cell Res.* **2007**, *20*, 301–304. [[CrossRef](#)]
59. Ladouce, M.; Barakat, T.; Su, B.L.; Deparis, O.; Mouchet, S.R. UV scattering by pores in avian eggshells. *Proc. SPIE* **2020**, *11481*, 101–109. [[CrossRef](#)]
60. Cockayne, E.I. The Distribution of Fluorescent Pigments in Lepidoptera. *Trans. R. Entomol. Soc. Lond.* **1924**, *72*, 1–19. [[CrossRef](#)]
61. Vukusic, P.; Hooper, I. Directionally Controlled Fluorescence Emission in Butterflies. *Science* **2005**, *310*, 1151. [[CrossRef](#)] [[PubMed](#)]
62. Israelowitz, M.; Rizvi, S.H.; von Schroeder, H.P. Fluorescence of the “fire-chaser” beetle *Melanophila Acuminata*. *J. Lumin.* **2007**, *126*, 149–154. [[CrossRef](#)]
63. Trzeciak, T.M.; Wilts, B.D.; Stavenga, D.G.; Vukusic, P. Variable multilayer reflection together with long-pass filtering pigment determines the wing coloration of papilionid butterflies of the *Nireus* Group. *Opt. Express* **2012**, *20*, 8877–8890. [[CrossRef](#)]
64. Hooijdonk, E.V.; Vandenbem, C.; Berthier, S.; Vigneron, J.P. Bi-functional photonic structure in the *Papilio Nireus* (Papilionidae): Model. Scatt.-Matrix Opt. Simulations. *Opt. Express* **2012**, *20*, 22001–22011. [[CrossRef](#)]
65. Van Hooijdonk, E.; Berthier, S.; Vigneron, J.P. Contribution of both the upperside and the underside of the wing on the iridescence in the male butterfly *Troides Magellanus* (Papilionidae). *J. Appl. Phys.* **2012**, *112*, 074702. [[CrossRef](#)]
66. Welch, V.L.; Van Hooijdonk, E.; Intrater, N.; Vigneron, J.P. Fluorescence in insects. *Proc. SPIE* **2012**, *8480*, 848004. [[CrossRef](#)]
67. Wilts, B.D.; Trzeciak, T.M.; Vukusic, P.; Stavenga, D.G. Papiliochrome II pigment reduces the angle dependency of structural wing colouration in *Nireus* Group Papilionids. *J. Exp. Biol.* **2012**, *215*, 796–805. [[CrossRef](#)]
68. Van Hooijdonk, E.; Barthou, C.; Vigneron, J.P.; Berthier, S. Yellow structurally modified fluorescence in the longhorn beetles *Celosterna pollinosa sulfurea* and *Phosphorus virescens* (Cerambycidae). *J. Lumin.* **2013**, *136*, 313–321. [[CrossRef](#)]
69. Mouchet, S.R.; Kaczmarek, A.M.; Mara, D.; Deun, R.V.; Vukusic, P. Colour and fluorescence emission of *Euchroea Auripigmenta* Beetle. *Proc. SPIE* **2019**, *10965*, 72–82. [[CrossRef](#)]
70. Mouchet, S.R.; Verstraete, C.; Kaczmarek, A.M.; Mara, D.; van Cleuvenbergen, S.; Van Deun, R.; Verbiest, T.; Maes, B.; Vukusic, P.; Kolaric, B. Unveiling the nonlinear optical response of *Trictenotoma Child*. Longhorn Beetle. *J. Biophotonics* **2019**, *12*, e201800470. [[CrossRef](#)] [[PubMed](#)]
71. Mouchet, S.R.; Verstraete, C.; Bokic, B.; Mara, D.; Dellieu, L.; Orr, A.G.; Deparis, O.; Deun, R.V.; Verbiest, T.; Vukusic, P.; et al. Naturally occurring fluorescence in transparent insect wings. *arXiv* **2021**, arXiv:2110.06086.
72. Lawrence, R.F. Fluorescence in Arthropoda. *J. Entomol. Soc. S. Afr.* **1954**, *17*, 167–170.
73. Pavan, M.; Vachon, M. Sur l'existence d'une substance fluorescente dans les téguments des Scorpions (Arachnides). *Comptes Rendus L'Académie Sci.* **1954**, *239*, 1700–1702.
74. Tani, K.; Watari, F.; Uo, M.; Morita, M. Fluorescent Properties of Porcelain-Restored Teeth and Their Discrimination. *Mater. Trans.* **2004**, *45*, 1010–1014. [[CrossRef](#)]

75. Taboada, C.; Brunetti, A.E.; Pedron, F.N.; Carnevale Neto, F.; Estrin, D.A.; Bari, S.E.; Chemes, L.B.; Peporine Lopes, N.; Lagorio, M.G.; Faivovich, J. Naturally occurring fluorescence in frogs. *Proc. Natl. Acad. Sci. USA* **2017**, *114*, 3672–3677. [[CrossRef](#)]
76. Deschepper, P.; Jonckheere, B.; Matthys, J. A Light in the Dark: The Discovery of Another Fluorescent Frog in the Costa Rican Rainforests. *Wilderness Environ. Med.* **2018**, *29*, 421–422. [[CrossRef](#)]
77. Mohd Top, M.; Puan, C.L.; Chuang, M.F.; Othman, S.N.; Borzée, A. First record of ultraviolet fluorescence in the Bent-toed Gecko *Cyrtodactylus Quadrivirgatus* Taylor, 1962 (Gekkonidae: Sauria). *Herpetol. Notes* **2020**, *13*, 211–212.
78. Gruber, D.F.; Gaffney, J.P.; Mehr, S.; DeSalle, R.; Sparks, J.S.; Platasa, J.; Pieribone, V.A. Adaptive Evolution of Eel Fluorescent Proteins from Fatty Acid Binding Proteins Produces Bright Fluorescence in the Marine Environment. *PLoS ONE* **2015**, *10*, e0140972. [[CrossRef](#)]
79. Gruber, D.F.; Loew, E.R.; Deheyn, D.D.; Akkaynak, D.; Gaffney, J.P.; Smith, W.L.; Davis, M.P.; Stern, J.H.; Pieribone, V.A.; Sparks, J.S. Biofluorescence in Catsharks (Scyliorhinidae): Fundamental Description and Relevance for Elasmobranch Visual Ecology. *Sci. Rep.* **2016**, *6*, 24751. [[CrossRef](#)] [[PubMed](#)]
80. Iriel, A.; Lagorio, M.G. Is the flower fluorescence relevant in biocommunication? *Naturwissenschaften* **2010**, *97*, 915–924. [[CrossRef](#)] [[PubMed](#)]
81. Iriel, A.; Lagorio, M.G. Implications of reflectance and fluorescence of *Rhododendr. Indicum* Flowers Biosignaling. *Photochem. Photobiol. Sci.* **2010**, *9*, 342–348. [[CrossRef](#)] [[PubMed](#)]
82. Purcell, E.M. Spontaneous emission probabilities at radio frequencies. *Phys. Rev.* **1946**, *69*, 681.
83. Yablonoivitch, E. Inhibited Spontaneous Emission in Solid-State Physics and Electronics. *Phys. Rev. Lett.* **1987**, *58*, 2059–2062. [[CrossRef](#)]
84. Kumazawa, K.; Tanaka, S.; Negita, K.; Tabata, H. Fluorescence from Wing of *Morpho Sulkowskyi* Butterfly. *Jpn. J. Appl. Phys.* **1994**, *33*, 2119–2122. [[CrossRef](#)]
85. Lawrence, C.R.; Vukusic, P.; Sambles, J.R. Grazing-incidence iridescence from a butterfly wing. *Appl. Opt.* **2002**, *41*, 437–441. [[CrossRef](#)]
86. Vigneron, J.P.; Kertész, K.; Vértesy, Z.; Rassart, M.; Lousse, V.; Bálint, Z.; Biró, L.P. Correlated diffraction and fluorescence in the backscattering iridescence of the male butterfly *Troides Magellanus* (Papilionidae). *Phys. Rev. E* **2008**, *78*, 021903. [[CrossRef](#)]
87. Van Hooijdonk, E.; Barthou, C.; Vigneron, J.P.; Berthier, S. Detailed experimental analysis of the structural fluorescence in the butterfly *Morpho Sulkowskyi* (Nymphalidae). *J. Nanophotonics* **2011**, *5*, 053525. [[CrossRef](#)]
88. Hooijdonk, E.V.; Barthou, C.; Vigneron, J.P.; Berthier, S. Angular dependence of structural fluorescent emission from the scales of the male butterfly *Troides Magellanus* (Papilionidae). *J. Opt. Soc. Am. B* **2012**, *29*, 1104–1111. [[CrossRef](#)]
89. Verbiest, T.; Kauranen, M.; Persoons, A.; Ikonen, M.; Kurkela, J.; Lemmetyinen, H. Nonlinear Optical Activity and Biomolecular Chirality. *J. Am. Chem. Soc.* **1994**, *116*, 9203–9205. [[CrossRef](#)]
90. Campagnola, P.J.; Millard, A.C.; Terasaki, M.; Hoppe, P.E.; Malone, C.J.; Mohler, W.A. Three-dimensional high-resolution second-harmonic generation imaging of endogenous structural proteins in biological tissues. *Biophys. J.* **2002**, *82*, 493–508. [[CrossRef](#)]
91. Friedl, P.; Wolf, K.; Harms, G.; Andrian, U.H. Biological Second and Third Harmonic Generation Microscopy. *Curr. Protoc. Cell Biol.* **2007**, *34*, 4.15.1–4.15.21. [[CrossRef](#)] [[PubMed](#)]
92. Ries, R.S.; Choi, H.; Blunck, R.; Bezanilla, F.; Heath, J.R. Black Lipid Membranes: Visualizing the Structure, Dynamics, and Substrate Dependence of Membranes. *J. Phys. Chem. B* **2004**, *108*, 16040–16049. [[CrossRef](#)]
93. Brown, D.J.; Morishige, N.; Neekhra, A.; Minckler, D.S.; Jester, J.V. Application of second harmonic imaging microscopy to assess structural changes in optic nerve head structure ex vivo. *J. Biomed. Opt.* **2007**, *12*, 5. [[CrossRef](#)]
94. Lis, D.; Guthmuller, J.; Champagne, B.; Humbert, C.; Busson, B.; Tadjeddine, A.; Peremans, A.; Cecchet, F. Selective detection of the antigenic polar heads of model lipid membranes supported on metals from their vibrational nonlinear optical response. *Chem. Phys. Lett.* **2010**, *489*, 12–15. [[CrossRef](#)]
95. Nguyen, T.T.; Conboy, J.C. High-Throughput Screening of Drug-Lipid Membrane Interactions via Counter-Propagating Second Harmonic Generation Imaging. *Anal. Chem.* **2011**, *83*, 5979–5988. [[CrossRef](#)]
96. Theer, P.; Denk, W.; Sheves, M.; Lewis, A.; Detwiler, P.B. Second-Harmonic Generation Imaging of Membrane Potential with Retinal Analogues. *Biophys. J.* **2011**, *100*, 232–242. [[CrossRef](#)]
97. Chen, X.; Nadiarynk, O.; Plotnikov, S.; Campagnola, P.J. Second harmonic generation microscopy for quantitative analysis of collagen fibrillar structure. *Nat. Protoc.* **2012**, *7*, 654. [[CrossRef](#)]
98. Akerboom, J.; Carreras Calderón, N.; Tian, L.; Wabnig, S.; Prigge, M.; Tolö, J.; Gordus, A.; Orger, M.B.; Severi, K.E.; Macklin, J.J.; et al. Genetically encoded calcium indicators for multi-color neural activity imaging and combination with optogenetics. *Front. Mol. Neurosci.* **2013**, *6*, 2. [[CrossRef](#)]
99. Rabasović, M.D.; Pantelić, D.V.; Jelenković, B.M.; Ćurčić, S.B.; Rabasović, M.S.; Vrbica, M.D.; Lazović, V.M.; Ćurčić, B.P.; Krmpot, A.J. Nonlinear microscopy of chitin and chitinous structures: A case study of two cave-dwelling insects. *J. Biomed. Opt.* **2015**, *20*, 016010. [[CrossRef](#)] [[PubMed](#)]
100. Chen, Y.C.; Lee, S.Y.; Wu, Y.; Brink, K.; Shieh, D.B.; Huang, T.D.; Reisz, R.R.; Sun, C.K. Third-harmonic generation microscopy reveals dental anatomy in ancient fossils. *Opt. Lett.* **2015**, *40*, 1354–1357. [[CrossRef](#)]
101. Lis, D.; Cecchet, F. Unique Vibrational Features as a Direct Probe of Specific Antigen–Antibody Recognition at the Surface of a Solid-Supported Hybrid Lipid Bilayer. *ChemPhysChem* **2016**, *17*, 2645–2649. [[CrossRef](#)] [[PubMed](#)]

102. Rowlands, C.J.; Park, D.; Bruns, O.T.; Piatkevich, K.D.; Fukumura, D.; Jain, R.K.; Bawendi, M.G.; Boyden, E.S.; So, P.T. Wide-field three-photon excitation in biological samples. *Light Sci. Appl.* **2017**, *6*, e16255. [[CrossRef](#)] [[PubMed](#)]
103. Reynaud, C.; Thoury, M.; Dazzi, A.; Latour, G.; Scheel, M.; Li, J.; Thomas, A.; Moulh erat, C.; Didier, A.; Bertrand, L. In-place molecular preservation of cellulose in 5,000-year-old archaeological textiles. *Proc. Natl. Acad. Sci. USA* **2020**, *117*, 19670–19676. [[CrossRef](#)]
104. Raoux, C.; Schmeltz, M.; Bied, M.; Alnawaiseh, M.; Hansen, U.; Latour, G.; Schanne-Klein, M.C. Quantitative structural imaging of keratoconic corneas using polarization-resolved SHG microscopy. *Biomed. Opt. Express* **2021**, *12*, 4163–4178. [[CrossRef](#)]
105. Schmeltz, M.; Robinet, L.; Heu-Thao, S.; Sint s, J.M.; Teulon, C.; Ducourthial, G.; Mahou, P.; Schanne-Klein, M.C.; Latour, G. Noninvasive quantitative assessment of collagen degradation in parchments by polarization-resolved SHG microscopy. *Sci. Adv.* **2021**, *7*, eabg1090. [[CrossRef](#)]
106. Mouchet, S.R.; Verstraete, C.; Mara, D.; Cleuvenbergen, S.V.; Finlayson, E.D.; Deun, R.V.; Deparis, O.; Verbiest, T.; Maes, B.; Vukusic, P.; et al. Nonlinear optical spectroscopy and two-photon excited fluorescence spectroscopy reveal the excited states of fluorophores embedded in a beetle’s elytra. *Interface Focus* **2019**, *9*, 20180052. [[CrossRef](#)]
107. Stoddart, P.R.; Cadusch, P.J.; Boyce, T.M.; Erasmus, R.M.; Comins, J.D. Optical properties of chitin: Surface-enhanced Raman scattering substrates based on antireflection structures on cicada wings. *Nanotechnology* **2006**, *17*, 680. [[CrossRef](#)]
108. Garrett, N.L.; Vukusic, P.; Ogrin, F.; Sirotkin, E.; Winlove, C.P.; Moger, J. Spectroscopy on the wing: Naturally inspired SERS substrates for biochemical analysis. *J. Biophotonics* **2009**, *2*, 157–166. [[CrossRef](#)]
109. Garrett, N.L. *Naturally Inspired SERS Substrates: Datasheet from Volume: “Raman Spectroscopy for Nanomaterials Characterization”*; SpringerMaterials: Cham, Switzerland, 2012. [[CrossRef](#)]
110. Garrett, N.L.; Sekine, R.; Dixon, M.W.A.; Tilley, L.; Bamberg, K.R.; Wood, B.R. Bio-sensing with butterfly wings: Naturally occurring nano-structures for SERS-based malaria parasite detection. *Phys. Chem. Chem. Phys.* **2015**, *17*, 21164–21168. [[CrossRef](#)] [[PubMed](#)]
111. Palmer, L.D.; Brooks, J.L.; Frontiera, R.R. Probing the coupling of butterfly wing photonic crystals to plasmon resonances with surface-enhanced Raman spectroscopy. *J. Mater. Chem. C* **2019**, *7*, 13887–13895. [[CrossRef](#)]
112. Langer, J.; Jimenez de Aberasturi, D.; Aizpurua, J.; Alvarez-Puebla, R.A.; Augu e, B.; Baumberg, J.J.; Bazan, G.C.; Bell, S.E.; Boisen, A.; Brolo, A.G.; et al. Present and Future of Surface-Enhanced Raman Scattering. *ACS Nano* **2020**, *14*, 28–117. [[CrossRef](#)] [[PubMed](#)]
113. Zhang, G.; Zhang, J.; Xie, G.; Liu, Z.; Shao, H. Cicada Wings: A Stamp from Nature for Nanoimprint Lithography. *Small* **2006**, *2*, 1440–1443. [[CrossRef](#)]
114. Dellieu, L.; Sarrazin, M.; Simonis, P.; Deparis, O.; Vigneron, J.P. A two-in-one superhydrophobic and anti-reflective nanodevice in the grey cicada *Cicada Orni* (Hemiptera). *J. Appl. Phys.* **2014**, *116*, 024701. [[CrossRef](#)]
115. Deparis, O.; Mouchet, S.R.; Dellieu, L.; Colomer, J.F.; Sarrazin, M. Nanostructured Surfaces: Bioinspiration for Transparency, Coloration and Wettability. *Mater. Today Proc.* **2014**, *1S*, 122–129. [[CrossRef](#)]
116. Kova evi , A.; Petrovi , S.; Mimidis, A.; Stratakis, E.; Panteli , D.; Kolaric, B. Molding Wetting by Laser-Induced Nanostructures. *Appl. Sci.* **2020**, *10*, 6008. [[CrossRef](#)]
117. Gao, T.; Zhu, X.; Wu, X.J.; Zhang, B.; Liu, H.L. Selectively Manipulating Upconversion Emission Channels with Tunable Biological Photonic Crystals. *J. Phys. Chem. C* **2021**, *125*, 732–739. [[CrossRef](#)]
118. Zhang, D. *Morphology Genetic Materials Templated from Nature Species*; Springer: Berlin/Heidelberg, Germany, 2012.